Condition Monitoring of Induction Motor Ball Bearing Using Monitoring Techniques

B.Hulugappa[*] , Tajmul Pashab[**], Dr.K.M.Ramakrishnac[***]

[*]Asst.Professor, Mechanical Engineering Department, NIE,Mysore, Karnataka
[**] Associate Professor, Mechanical Engineering Department , NIE,Mysore, Karnataka
[***]Professor, Mechanical Engineering Department, PESCE, Manday, Karnataka

Abstract- Rolling element bearings are critical components in induction motors and monitoring their condition is important to avoid failures. Several condition monitoring techniques for the bearings are available. Out of these, stator current monitoring is a relatively new technique. Vibration, stator current, acoustic emission and shock pulse methods (SPMs) and FEM, surface analysis, for the detection of a defect in the Inner race of induction motor ball bearing have been compared. The measurements were performed at different loads and different speeds. The defect in the bearing could be detected by all the methods.

I. INTRODUCTION

Induction motors are widely used in industry and are considered as critical components for electric utilities and process industries. In the case of induction motors, rolling element bearings are overwhelmingly used to provide rotor support. Although induction motors are reliable, they are subjected to some modes of failures .Based on studies according to Motor Reliability Working Group (MRWG) and the investigation carried out by Electric Power Research Institute (EPRI), a common mode of failure of an induction motor is the bearing failure followed by stator winding and rotor bar failures. The bearing failure increases the rotational friction of the rotor. Even under normal operating conditions of balanced load and good alignment, fatigue failure begins with small fissures, located below the surfaces of the raceway and rolling elements, which gradually propagate to the surface generating detectable vibrations and increasing noise levels. Continued stressing causes the fragments of the material to break loose producing localized fatigue phenomena known as flaking or spalling. Electric pitting or cracks due to excessive shock loading are also among the different types of bearing damage described in the literature [1,2]

The widespread application of rolling element bearings in both industry and commercial life require advanced technologies to efficiently and effectively monitor their health status. There are many condition monitoring methods used for detection and diagnosis of rolling element bearing defects: vibration measurements, temperature measurement, shock pulse method (SPM) and acoustic emission (AE). Among these vibration measurements are most widely used. Even though the emphasis is on vibration measurement methods, stator current harmonics measurement is appearing as an alternative to the vibration measurement methods. In fact, large electrical machine systems are often equipped with mechanical sensors, which are primarily vibration sensors such as proximity probes. However, these are delicate and expensive. Various researchers have suggested that stator current monitoring can provide the same indications without requiring access to the motor. This technique utilises results of spectral analysis of the stator current or supply current of an induction motor for the diagnosis [1].A detailed review of different vibration and acoustic methods, such as vibration measurements in time and frequency domains, sound measurement, the SPM and the AE technique for condition monitoring of rolling bearings have been presented by Tandon and Choudhury [3]. Each bearing has a characteristic rotational frequency. With a defect on particular bearing element, an increase in vibration energy at this element's rotational defect frequency may occur. These characteristic defect frequencies can be calculated from kinematics considerations, i.e. geometry of the bearing and its rotational speed. For normal speeds, the bearing characteristic defect frequencies lie in the low-frequency range and are usually less than 500 Hz.The relationship of the bearing vibration to the stator current spectra can be determined by remembering that any air gap eccentricity produces anomalies in the air gap flux density. Since ball bearings support the rotor, any bearing defect will produce a radial motion between the rotor and stator of the machine. Riley et al.[4] presented a method for sensor less on-line vibration monitoring of induction machines. This method assumed a linear relationship between the current harmonics and vibration level. Da-Ming Yang and JamesPenman [5] addressed the use of stator current and vibration monitoring to diagnose bearing condition. In their study it has been reported that monitoring of stator current provides an alternative method for diagnosing bearing condition that is generally less intrusive, simpler and successful detection of motor bearing condition is possible using line current sensing.

AE is the phenomena of transient elastic wave generation due to a rapid release of strain energy caused by structural alteration in a solid material under mechanical or thermal stresses. Generation and propagation of cracks are among the primary sources of AE in metals. AE transducers are designed to detect the very high frequency (450 kHz) stress waves that are generated when cracks extend under load. The most commonly measured AE parameters are peak amplitude, counts and events of the signal. Counts involve counting the number of times the amplitude exceeds a preset voltage level in a given time and gives a simple number characteristic of the signal. An event consists of a group of counts and signifies a transient wave. One of the advantages of AE monitoring is that it can detect the growth of subsurface cracks. Hence, it is an important tool for

condition monitoring. It has been shown that AE parameters can detect defects before they appear in the vibration acceleration [6–8]. Tandon and Nakra [9] demonstrated the usefulness of some AE parameters, such as peak amplitude and count, for detection of defects in radially loaded ball bearings at low and normal speeds. Tan [10] has presented the application of AE for the detection of bearing failures. He has suggested that the measurement of area under the amplitude curve is preferred method for detection of defects in rolling element bearings.

The shock pulses caused by the impacts in the bearings initiate damped oscillations in the transducer at its resonant frequency. Measurement of the maximum value of the damped transient gives an indication of the condition of rolling bearings. Low-frequency vibrations in the machine, generated by sources other than rolling bearings, are electronically filtered out. The maxim normalized shock value is a measure of the bearing condition. Shock pulse meters are simple to use so that semiskilled personnel can operate them. They give a single value indicating the condition of the bearing straightaway, without the need for elaborate data interpretation as required in some other methods.

The principle is based on the fact that structural resonances are excited in the high-frequency zone due to impulsive loading caused, for example, from spalling of the races or rolling elements and can be detected by a transducer whose resonance frequency is tuned to it. The SPM, which works on this principle, uses piezoelectric transducer having a resonant frequency based at 32 kHz[11,12]. In industries SPM has gained wide acceptance for detecting the rolling element bearing defects.

The literature indicates that even though the emphasis is on vibration measurement methods for the detection of defects in rolling element bearings in induction motor, stator current harmonics measurement can be an effective alternative to the vibration measurement because of its faster diagnosis. Very few studies have been carried out on stator current monitoring of an induction motor for the detection of defects in these rolling bearing along with vibration monitoring and other condition monitoring methods. Hence, there is a need for a comprehensive study of induction motor rolling element-bearing faults detection using stator current harmonics measurement in combination with vibration, AE and SPM condition monitoring techniques. So the present work was undertaken for the detection and diagnosis of induction motor rolling element-bearing faults have been carried out using vibration monitoring, AE and shock pulse along with stator current harmonics measurements. Experimental investigation has been carried out to study the changes in these parameters for bearings in good condition and with simulated defects in the outer race of the bearings of an induction motor.

II. Experimental set-up and measurements

2.1. Test rig

The test rig used in the present research work consists of a 1.1kW/1440 rpm single-phase induction motor driving the V-belt drive. The test bearing is the drive end bearing of induction motor, housed within the drive end cover plate of motor to support rotor. The rotor shaft of motor is extended to the left of drive end cover plate of motor for providing transmission of power through pulley drive. The test bearing can be radial loaded with V-belt drive with the loading system. Vibration isolation rubber sheets were provided under the motor and its supporting legs to reduce the vibration transmission from ground to the test bearing. The drive to the induction motor is provided by a.c. power supply. The transducers for measurement of vibration, AE and SPM have been mounted in the zone of maximum load on to the drive end bearing of induction motor. The Schematic diagram of the experimental set-up is shown in Fig. 1. The test rig has been designed to withstand a maximum load of 27 kg based on the rated power of induction motor for 1.5 HP. The test bearing of induction motor in this study is normal clearance, deep groove ball bearings SKF 6205. Equal amount of SKF grease (4 g) was applied to the bearing, which was immersed in kerosene and finally cleaned with acetone to remove preserving oil.

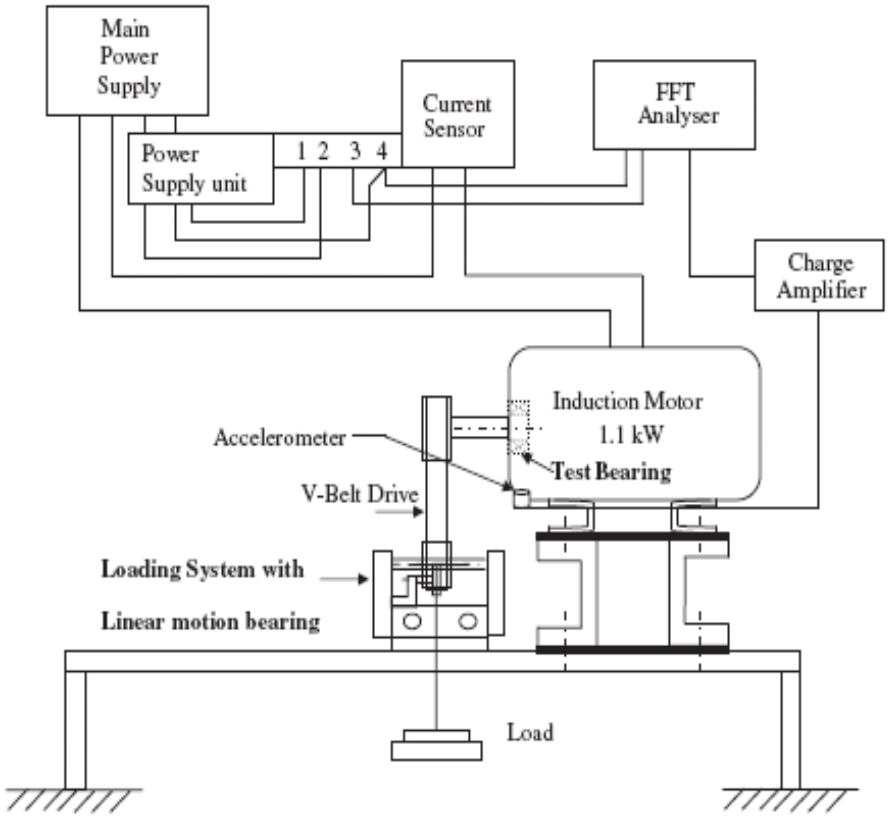

Fig. 1. Schematic diagram of test rig.

2.2. Instrumentation

Vibrations were measured with the help of a piezoelectric accelerometer Bruel and Kjaer (B&K) type 4366having un damped natural frequency of 39 kHz. The output of the accelerometer was fed to the B&K charge amplifier 2635 connected to Ono Sokki CF 3200 portable fast Fourier transform analyzer. The schematic diagram of the current sensor(working on Hall effect) in series with motor supply line is shown in Fig. 1. The Hall element located in the air gap of the magnetic circuit converts the magnetic field generated by the primary current into a proportional Hall voltage. The magnetic field produced by the primary current generates a highly linear magnetic flux in the air gap of the magnetic circuit, which in turn induces a proportional Hall voltage in the Hall element. The voltage is then electronically amplified resulting in an output voltage that is highly proportional to the primary current up to the final value of the measuring range. The current sensor is supplied with 715V from the power supply unit for 15min before taking the measurements.

The current flowing in single-phase induction motor was sensed by a current sensor of type LEM-HY 25P by connecting it in series with the supply line to the motor. This current sensor has dynamic performance accuracy of linearity better than 70.2%, response time better than 1 ms and nominal analog output current 25 mA. The output from the current sensor is fed to the FFT analyzer with frequency span of500 Hz and 20 kHz for frequency spectrum analysis and for overall values, respectively.AE measurements were performed by using Acoustic Emission Technology Corporation (AET), model AET AC 375 L transducer which are of same frequency of 375 kHz, a preamplifier with 60 dB gain (AET 160B)and a filter (AET FL 25) with a pass band of 250–500 kHz. The AE transducer was mounted on the test bearing housing with grease as couplant and with the help of cloth adhesive tape. The preamplifier is provided with 712V DC supply. The output from the preamplifier was fed to Tektronix TDS 210 digital real time oscilloscope, which can also give frequency spectrum.

The Shock Pulse Tester T2000 by SPM Instrument AB, Sweden, along with its hand held transducer type SPM 10777 was used for shock pulse measurements. The hand held probe was pressed straight at the zone of maximum load on bearing housing to get maximum normalized shock pulse value, dBM.

2.3. Measurement conditions

The measurements were carried out from no load to full load (27 kg) for the induction motor bearing with an increment of 5 kg. The motor was run at constant speed of 1440 rpm. Three healthy bearings were used to check the repeatability of the measurements. Inner race defect was simulated by a circular hole of diameter varying from 250 to 1500 mm in the outer race of the same bearing (in steps of 250 mm successively after each measurement) by spark erosion technique.

III. RESULTS AND DISCUSSIONS

3.1. Vibration velocity

Fig. 2 shows that the overall amplitudes of vibration velocity of three healthy bearings are very much close to each other and their average overall level is also shown. Fig. 3 shows that overall velocity values follow the same trend as that of the good bearing with increase in load. The overall velocity value has increased even for a small defect size of 250 mm. The overall velocity significantly increases to 66% in case of a maximum defect size of 1500 mm with respect to healthy bearing at 15 kg load. The spectrum of the vibration velocity signal in the low-frequency range was obtained to observe changes at the characteristic defect frequency of the bearing outer race due to defects in it. The characteristic defect

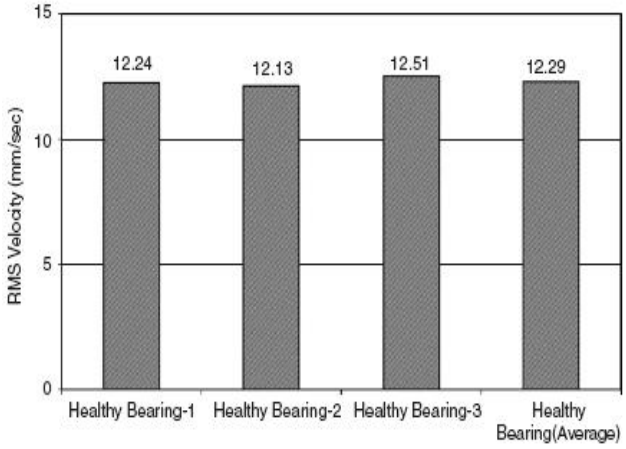

Fig. 2. Vibration velocity of healthy bearings at 15kg load.

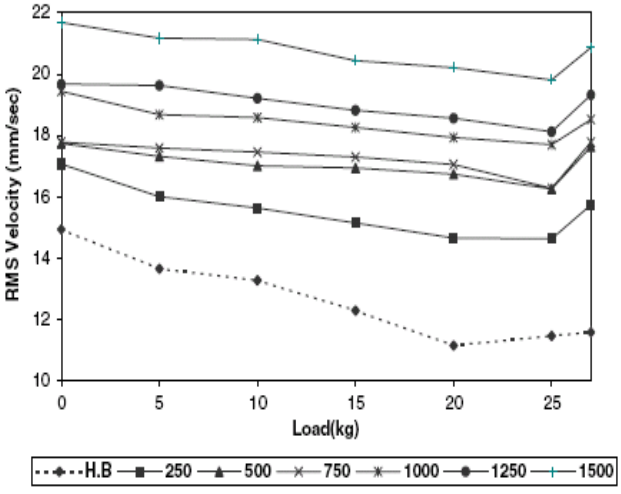

Fig. 3. Overall vibration velocity with outer race defects.

frequency of the rolling element bearing outer race can be calculated by using the following equation [3,13]:

$$fo(HZ)=N/2f_r[1-bd/pd\ Cos\beta) \quad (1)$$

where f_r is the shaft rotational frequency, N is number of balls, bd and pd are the ball diameter and pitch circle diameter ,respectively, and b is the contact angle of the ball (with the races). For the shaft rotational frequency f_r= 24 Hz and a test bearing having nine balls of diameter 8.5mm and pitch circle diameter of 38.5mm with contact angle ß=0, the characteristic inner race defect frequency fo is found to be84.15 Hz.

Velocity spectrum of one of the healthy bearings in the low-frequency range of 500 Hz at 15 kg load is shown in Fig. 4.From the spectrum of velocity, it has been observed that the peak occurs at fundamental frequency of shaft (i.e. at 24 Hz) and at twice the supply frequency (i.e. at 100 Hz) in the spectral component

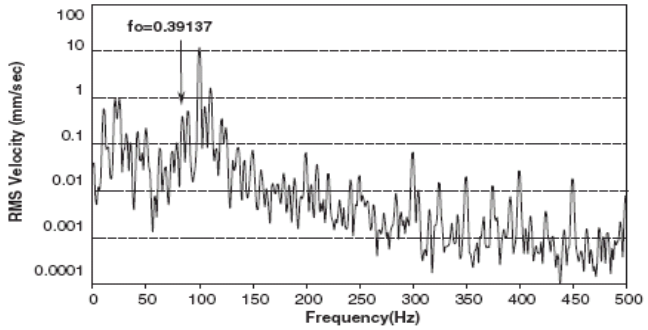

Fig. 4. Spectrum of vibration velocity of healthy bearing.

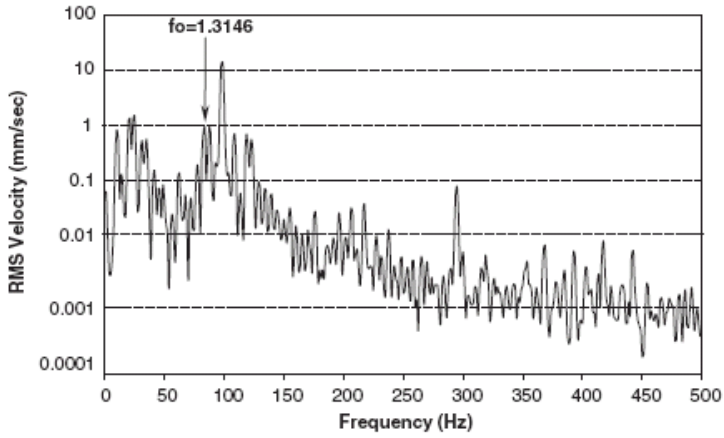

Fig. 5. Spectrum of vibration velocity for 1500µm defect.

3.2. Stator current signals

Fig. 6 shows the overall value of stator current amplitude comparison at 15 kg load for 0–20 kHz range of three healthy bearings and also the average overall stator current of three healthy bearings. From this chart also it is observed that the overall amplitudes are very much close tone another for the three healthy bearings. The overall stator current values were taken for all the defect sizes in the inner race of the bearing. Fig. 7 shows that the overall stator current values follow the same trend as that of the good bearing within crease in load. The overall stator current value has increased slightly even for a small defect size of 250 mm. From 250 to 1250 mm, the amplitude of overall stator current values increase continuously and the increase is much more for 1500 mm defect size. As mentioned in the

literature, a defect in rolling element-bearing causes an increase in the overall RMS value of stator current for a known frequency range. Hence, the results obtained from the stator current correlates with the results reported in [4,15].

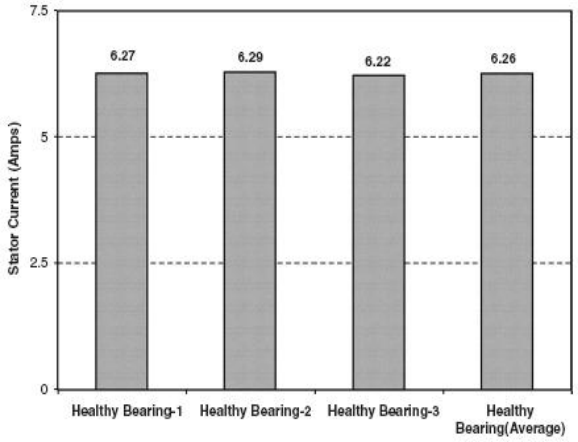

Fig. 6. Overall stator current of healthy bearings at 15kg load.

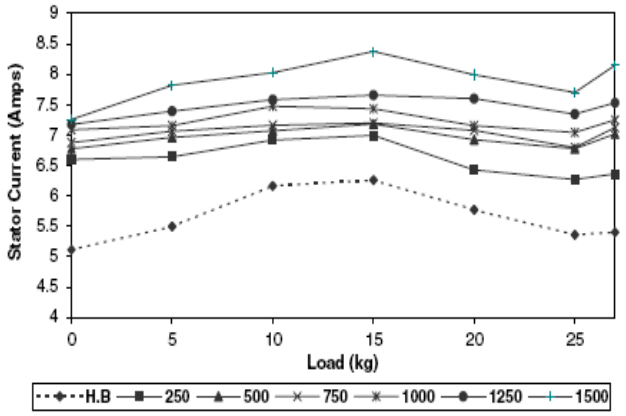

Fig. 7. Overall stator current with outer race defects.

Thus, overall stator current has appreciably increased by 39.79% in case of maximum defect size of 1500 mm with respect to healthy bearing at15 kg load. The relationship of the bearing vibration to the stator current spectra can be determined by remembering that any air gap eccentricity produces anomalies in the air gap flux density [13]. Since ball bearings support the rotor, any bearing defect will produce a radial motion between the rotor and stator of the machine. The mechanical displacement resulting from damaged bearing causes the machine air gap to vary in a manner that can be described by combinations of rotating eccentricities moving in both directions [16]. Thus, bearing fault simulated in the inner race of the bearing may also cause rotor eccentricity, which is one of the common mechanical faults in the bearing. The rotor eccentricity in induction motor takes two forms, i.e. static eccentricity (where the rotor is displaced from the stator bore centre but still rotating upon its own axis) and dynamic eccentricity (where the rotor is still turning upon the stator bore centre but not on its own centre).Eccentricity causes a force on the rotor that tries to pull the rotor even further from the stator bore centre. In the case of static eccentricity this is a steady pull in one direction. This makes the unbalanced magnetic pull(UMP) difficult to detect unless specialist experimental equipment is utilized, which is not possible for motors in service. Dynamic eccentricity produces a UMP, which acts on the rotor and rotates at rotor rotational velocity.

Both types of eccentricities cause excessive stressing of the machine and greatly increase bearing wear due to uneven magnetic pull produced that leads to variation of the sideband current magnitudes or predicted current harmonics in relation to vibration velocity. Hence, any fault condition in the induction motor causes the magnetic field in the air gap of the machine to be non-uniform. It has been shown by Schoen [1] that these vibration frequencies reflect themselves in the current spectrum as f bng=[fe± mfv] (2)
where fe is the electrical supply frequency, m =1,2,3… is one of the characteristic vibration frequencies. A current signal of a single phase of stator current of induction motor and a vibration signal from a vibration sensor located at the bearing housing of induction motor for three good bearings were obtained. The corresponding current spectrum components in relation to vibrations for the supply frequency fe of 50 Hz and at characteristic outer race defect vibration frequency of 84.15 Hz are 34.15 and 134.15 Hz. Fig. 8 shows the acquired current spectrum for the same low-frequency range of 500 Hz at 15 kg load as that of vibration velocity spectrum to verify the relationship between stator current and vibration velocity for healthy bearing. The spectrum of stator current in Fig. 8 indicates peak at supply frequency of 50 Hz in the current spectrum, whereas at twice the supply frequency in the velocity spectrum (Fig. 4) indicating the UMP even under normal operating condition. The corresponding current spectrum components in relation to vibrations were not significant at
[f e _ f o](i.e. at 34.15 Hz) and [fe+fo] (i.e. at 134.15 Hz) as shown in Fig. 8.

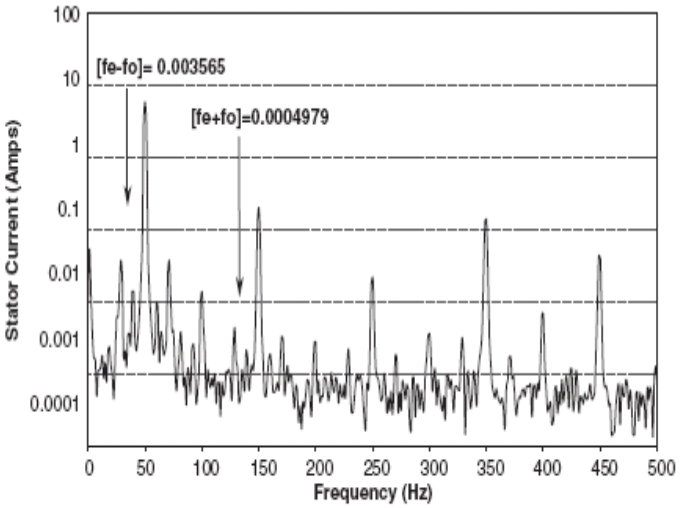

Fig. 8. Spectrum of stator current of healthy bearing.

The rest of the peak component other than at 50 Hz present in the current spectrum occur at multiples of the supply frequency and these are caused due to saturation, winding distribution and supply voltage. The stator current spectrum of motor with the outer race defect of the bearing from 250 to 1500 mm in steps of 250 mm were obtained in the low frequency of 500 Hz for 15 kg load and the plot of 1500 mm is shown in Fig. 9. Predicted current harmonics for outer race of the bearing relating vibration characteristic defect frequencies with the supply current frequency are compared with those of healthy bearing. For minimum defect size in the outer race of the bearing of motor, there was marginal increase in the amplitude of the predicted current harmonics component at [f e - f o]=34:15 Hz and[f e + f o]=134:15 Hz. However, significant increase in the amplitude of predicted current harmonics or vibration sideband current magnitudes is observed as the defect size increases as shown in Fig. 9. These results are comparable with results reported in [5,13,17]for the outer race defect in the bearing.

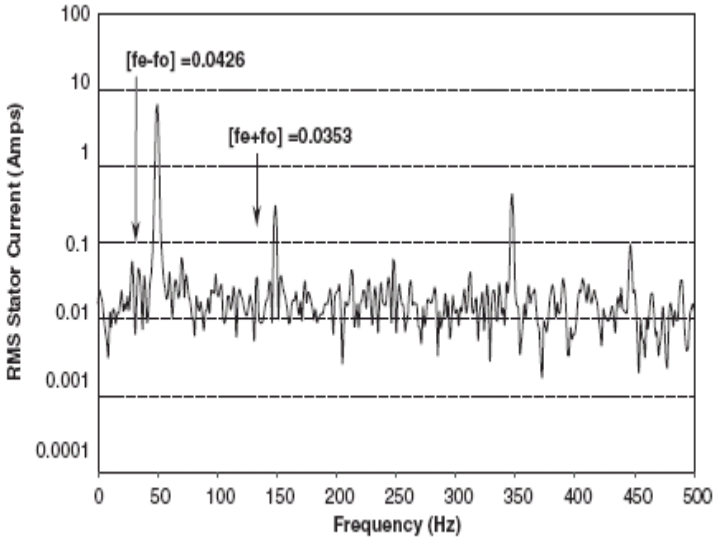

Fig. 9. Spectrum of stator current for 1500 µm defect.

3.3. Acoustic emission monitoring

In the present work, peak amplitudes of the AE signal of three healthy bearings from no load to full load were obtained. Peak amplitudes of the signal at 375 kHz were obtained and are expressed in dB with 0 dB corresponding to 1 Vrms in the oscilloscope. The values of AE maximum peak amplitude of three healthy bearings are shown in Fig. 10. The average value is 31.8 dB. Fig. 11 shows the AE maximum peak amplitude obtained from no load to full load for all defect sizes in the outer race of the bearing. It is observed that as the defect size increases the peak amplitude also increased. It has been observed from Fig. 11; the peak amplitude increased till 10 kg load and then decreases slightly with increase in load. The range of AE maximum peak amplitudes from healthy bearing to maximum defect size are 31.4–67.8 dB at 10 kg load and 31.8–63.2 dB at15 kg load. In general the difference in A maximum peak amplitude of healthy and smallest defect size is quite significant and makes it possible to detect the presence of a defect for diagnosis easier at the early stage in comparison with other condition monitoring techniques. There is an appreciable increase of 98.74% in case of maximum defect size with respect to healthy bearing at 15 kg load. Whereas for 10 kg load, the increase is115.92% in case of maximum defect size with respect to healthy bearing.

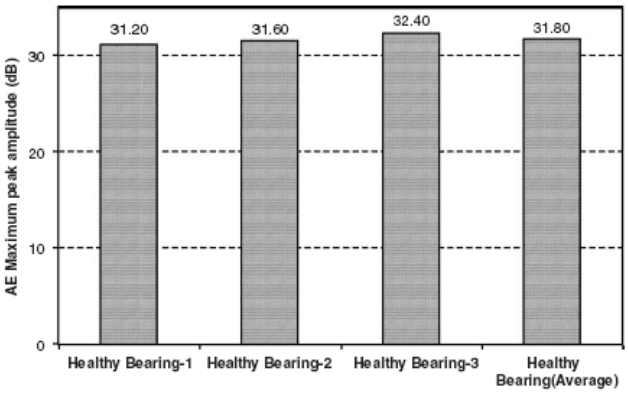

Fig. 10. Acoustic emission peak amplitude of healthy bearings at 15 kg load.

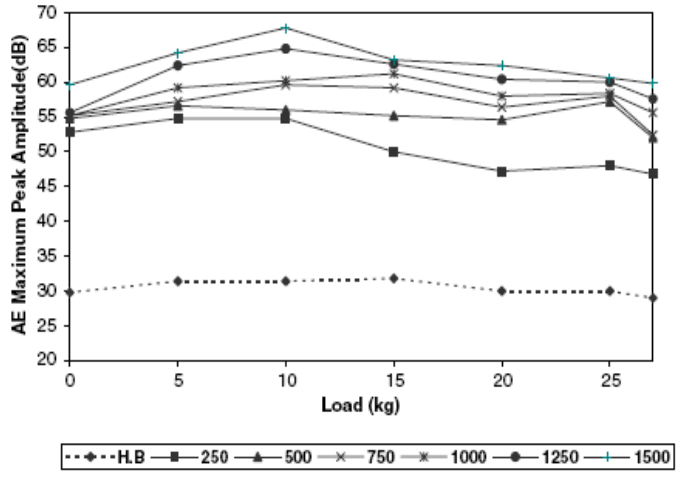

Fig. 11. Acoustic emission peak amplitude with outer race defects.

3.4. Shock pulse method (SPM)

To neutralize the effect of rolling velocity on the measured value, the instrument was fed the shaft diameter of 25mm and rotational speed of 1440 rpm. After this SPM T2000 series calculates the initial shock value dBi, and displays maximum normalized shock pulse values. Fig. 12 shows the comparison chart for maximum normalized value and average value of three healthy bearings. The values vary from 14

to 17 dB and are less than 20, indicating good bearing condition. Maximum normalized values (dBM) obtained for all defect sizes of250–1500 mm in the outer race of the bearing from no load to full load at constant motor speed are given in Fig. 13 in comparison with the average value of three healthy bearings. It is seen that the levels for different bearings are more than that of healthy bearing and for 250–750 mm defect size, values of dBM are greater than20 and less than 35. For the defect size greater than 750 mm values of dBM are greater than 35. The dBM obtained indicates caution zone for the defect size of 250–750 mm and for the defect size above 750 mm dBM values obtained indicate the damaged bearing condition. Maximum normalized value as high as 50 was measured for the maximum defect size.

IV. Comparison of Techniques

The comparative study of different condition monitoring techniques has been done for minimum and maximum defect size in the outer race of the bearing. Fig. 14 shows the effectiveness of each technique in terms of percentage increase with respect to average value of healthy bearing, for the smallest defect size. As seen in Fig. 14, AE technique is the most effective technique followed by SPM. The maximum normalized value of SPM is almost three times less effective as compared to AE technique. Overall vibration velocity and stator current come in the third and fourth place, respectively. Fig. 15 shows the same order in the effectiveness of each technique for maximum defect size. However, stator current monitoring has the advantage that it requires minimum instruments and is sometimes referred to as sensor less technique.

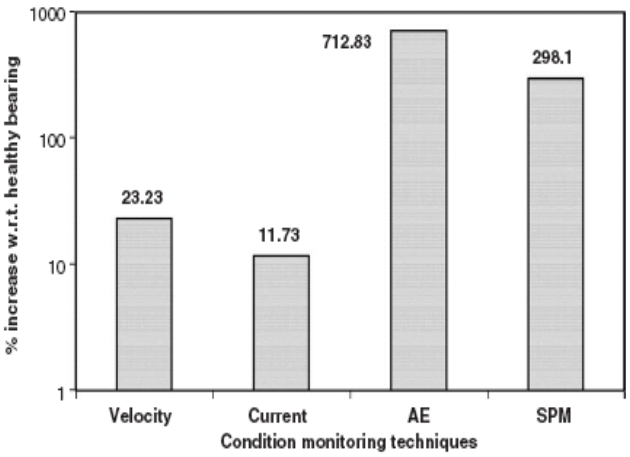

Fig. 14. Comparison of condition monitoring techniques for minimum defect size.

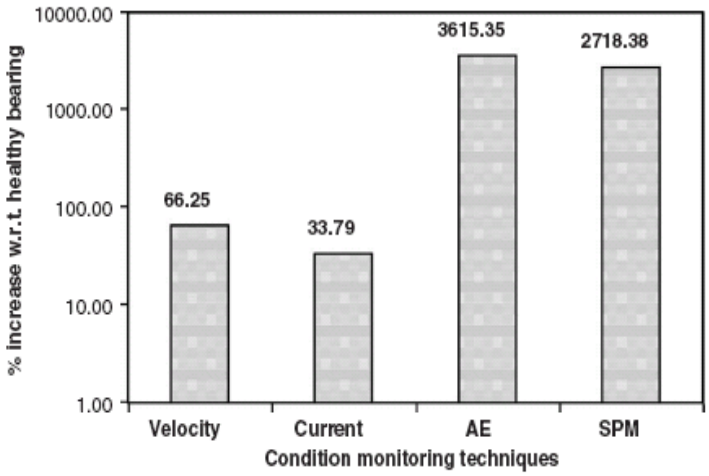

Fig. 15. Comparison of condition monitoring techniques for maximum defect size.

V. Conclusions

The vibration and stator current signal measurements performed on the bearing of an induction motor are successful in detecting simulated defects in the outer race of the bearing. Current harmonics for bearing outer race defect characteristic vibration frequency has shown significant increase in the current spectrum components for maximum size of defect. The AE and SPM measurement performed are very good in detecting the bearing defect. On comparing the results of good and defective bearing, it is observed that AE peak amplitude and shock pulse maximum normalized value level increase much more than other techniques as defect size increases. AE monitoring has proved to be the best technique. Stator current monitoring is perhaps the most cost-effective technique.

References

[1] R.R. Schoen, B.K. Lin, T.G. Habetler, J.H. Schlag, S. Farag, An unsupervised, on-line system for induction motor fault detection using stator current monitoring, IEEE Transactions on Industry Applications 31 (6) (2007) 1280–1286.

[2] F.F. Albrechi, J.C. Apparatus, R.M. McCoy, E.L. Owen, D.K. Sharma, Assessment in the reliability of motors in utility application—updated, IEEE Transactions on Energy Conversion 1 (1) (2009) 39–46.

[3] N. Tandon, A. Choudhury, A review of the vibration and acoustic measurement methods for detection of defects in rolling elementbearings, Tribology International 32 (8) (1999) 469–480.

[4] C.M. Riley, B.K. Lin, T.G. Hebelter, R.R. Schoen, A method for sensor-less on line vibration monitoring of induction machines,IEEE Transactions on Industry Applications 34 (6) (2008) 1240–1245.

[5] Y. Da-Mang, P. James, Intelligent detection of induction motor bearing faults using current and vibration monitoring, in:Proceedings ‘‘COMADEM 2000’’, 3–8 December 2000, pp. 461–470.

[6] T. Yoshioka, T. Fuhjiwara, Application of acoustic emission technique to detection of rolling element-bearing failure, in:D.A. Dornfield (Ed.), Acoustic Emission Monitoring and Analysis in Manufacturing, ASME, New York, 2010, pp. 55–75.

[7] T. Yoshioka, Detection of rolling contact subsurface fatigue cracks using acoustic emission technique, Lubrication Engineering 49 (4)(2012) 303–308.

[8] T. Yoshioka, M. Takeda, Classification of rolling contact fatigue initiation using acoustic emission technique, LubricationEngineering 51 (1) (2004) 41–44.

[9] N. Tandon, B.C. Nakra, Defect detection in rolling element bearings by acoustic emission method, Journal of Acoustic Emission 9 (1)(1990) 25–28.

[10] C.C. Tan, Application of acoustic emission to the detection of bearing failures, in: Proceedings ‘‘Tribology Conference’’, Brisbane,1990, pp. 110–114.

[11] D.E. Butler, The shock pulse method for the detection of damaged rolling bearings, NDT International 6 (2) (2010) 92–95.

[12] I.E. Morando, Measuring shock pulses is ideal for bearing condition monitoring, Pulp and Paper 62 (12) (2008) 96–98.

[13] R.R. Schoen, T.G. Habetler, F. Kamran, R.G. Barthheld, Motor bearing damage detection using stator current monitoring, IEEETransactions on Industry Applications 31 (6) (2005) 1274–1279.

[14] N. Tandon, B.C. Nakra, Detection of defects in rolling element bearings by vibration monitoring, Journal of Institution of Engineers(India), Mechanical Engineering Division 73 (2003) 271–282.

[15] M. El Hachemi Benbouzid, A review of induction motor signature analysis as a medium for fault detection, IEEE Transactions onIndustrial Electronics 47 (5) (2000) 984–993.

[16] C.M. Riley, B.K. Lin, T.G. Habetler, G.B. Kliman, Stator current harmonics and their casual vibrations: a preliminary investigationof sensor less vibration monitoring applications, IEEE Transactions on Industry Applications 35 (1) (1999) 94–99.

[17] M. El Hachemi Benbouzid, M. Vieira, C. Theyes, Induction motors’ faults detection and localization using stator current advancedsignal processing techniques, IEEE Transactions on Power Electronics 14 (1) (2009) 14–22.

AUTHORS

First Author – B.Hulugappa, Asst.Professor, Mechanical Engineering Department, NIE,Mysore, Karnataka , bhniemech@gmail.com

Second Author – Tajmul Pasha, Associate Professor, Mechanical Engineering Department , NIE,Mysore, Karnataka, tpniemech@gmail.com

Third Author – Dr.K.M.Ramakrishn, Professor, Mechanical Engineering Department, PESCE, Manday, Karnataka

Correspondence Author – B.Hulugappa.9481439473